JOURNAL OF PROPULSION AND POWER
Vol. 23, No. 6, November–December 2007

Microscale Thrusters with Pulsed Optical Lattices/Gas Nonresonant Dipole Interaction

Mikhail N. Shneider*
Princeton University, Princeton, New Jersey 08544
and
Cedrick Ngalande† and Sergey F. Gimelshein‡
University of Southern California, Los Angeles, California 90089

DOI: 10.2514/1.23975

The direct simulation Monte Carlo method is used to study the feasibility of new propulsion concepts based on the interaction of an optical lattice with gas molecules. Two regimes are considered, high density and low density. In the first one, a de Laval nozzle is examined with the carrier gas driven by energy and momentum deposition from the lattice to the region near the nozzle throat. Analytical expressions are developed and compared with the numerical predictions that describe the energy and momentum energy transfer between the lattice and the gas. In the second regime, a multiple orifice flow is considered with molecules accelerated to high velocities by a chirped lattice potential. Specific impulse of about 500 is obtained with the total thrust of over 10 μN per single 100 μm orifice.

Nomenclature

a = acceleration, m/s^2
c = speed of light, m/s
E = amplitude of the optical electric field, V/m
$\bar{E}$ = normalized energy, K
F = force, N
F_x = longitudinal force, N/m^3
f = molecular velocity distribution function
I_{sp} = specific impulse, s
I = laser intensity, W/m^2
I_{max} = maximum pulse intensity, W/m^2
k = wave number, 1/m
k_B = Boltzmann constant, J/K
l_c = gas mean free path, m
m = mass of molecules, kg
N = gas density, molecule/m^3
n = index of refraction
P_d = power transferred to gas from the lattice, W/m^3
q = lattice wave number, 1/m
T = temperature, K
t = time, s
$\bar{t}$ = nondimensional time
v = molecule velocity, m/s
W = density of electromagnetic energy in the lattice, J/m^3
X_c = lattice center location, m
x = distance, m
$\bar{x}$ = nondimensional distance, m
Z_0 = impedance of vacuum, Ω
α = static molecular polarizability, A^2 s^2 kg^{-1}
β = frequency chirp, rad/s^2
Δp = momentum change per molecule, kg · m/s
$\Delta\varpi$ = energy change per molecule, J
ϵ_0 = permittivity of free space, F/m
Θ = density of momentum per unit volume, kg/(m^2 s)
λ = spatial period of the optical lattice potential, m
μ_0 = permeability of free space, H/m
ξ = phase velocity, m/s
τ_{col} = collision time, s
ϕ_m = lattice potential well depth, J
ω = laser frequency, rad/s

Subscript

0 = initial state
1, 2 = laser beams 1 and 2

I. Introduction

AN OPTICAL lattice, which represents a periodic optical dipole potential, is created by the interaction between a polarizable particle and the field of an optical interference pattern formed by counterpropagating laser fields. Optical dipole potentials have been used extensively to trap and manipulate ultracold atoms in the nK–μK range using the optical dipole force. Although these conservative optical forces are weak, they are capable of trapping ultracold atoms [1,2] and have been used to guide atoms through optical fibers [3]. Larger potentials in the 100 K range can be produced by high-intensity pulsed lasers for shorter time periods where the maximum potential is limited by the probability of multiphoton dissociation and ionization at high laser intensities. These stronger potentials have been used to deflect cold molecules, ~5 K, and, more recently, to dissociate diatomic molecules by strong centrifugal optical forcing [4].

Synchronous acceleration of charged particles to energies in excess of 100 GeV can be achieved using electrostatic and Lorentz forces, and accelerated neutral atomic beams can be created from ion beams by charge capture [5]. Gas dynamic methods that accelerate molecules to velocities greater than 10 km/s (14.5 eV for N_2) [6] have been demonstrated, but it is extremely challenging to accelerate neutral molecules above this energy range without a large fraction of the gas being thermally ionized and dissociated.

Linear acceleration within the time-varying electric field of an accelerated optical traveling wave has been proposed as a means to accelerate atoms to high velocities [7,8], and, more recently, molecular acceleration has been proposed [9]. Linear acceleration using optical fields is attractive because extremely large dipole forces

Presented as Paper 0768 at the 44th AIAA Aerospace Sciences Meeting and Exhibit, Reno, NV, 9–12 January 2006; received 16 March 2006; revision received 3 July 2007; accepted for publication 10 July 2007.

*Research Scientist, Department of Aerospace and Mechanical Engineering. Senior Member AIAA.
†Graduate Student, Department of Aerospace and Mechanical Engineering.
‡Research Assistant Professor, Department of Aerospace and Mechanical Engineering. Member AIAA.

can be produced by high electric field gradients that can be created within an optical traveling wave. The electrodeless electric field gradient produced by a focused laser beam can be orders of magnitude greater than electrostatic gradients, allowing acceleration of not only polar, but also polarizable, molecules and atoms. This concept has already been demonstrated with acceleration of ultracold atoms up to the velocities in the meter-per-second range using very weak optical periodic potentials, which are called optical lattices [10,11]. A one-dimensional optical lattice was created by two counterpropagating laser beams, and acceleration of the lattice was achieved by changing the frequency of the counterpropagating fields (chirping) with respect to time.

In contrast to acceleration of ultracold atoms in weak lattices [10,11], the authors of [12,13] have studied the acceleration of polarizable gas particles, both molecules and atoms, at much higher temperatures (5–300 K) and to velocities in the 10–100 km/s range by application of large lattice potentials created by pulsed lasers. The latter work follows on from the original work of Kazantsev [7,8], and investigates the motion of trapped and untrapped particles in the velocity phase space of the accelerated optical dipole potential. The dynamics of the accelerating ensemble of polarizable particles under the influence of large dipole or stark forces is examined, and the velocity distribution function of both trapped and untrapped particles is predicted [12].

Recently, the molecular beam formation was also demonstrated in the collisional regime (pressures 400 and 1300 Pa) by the direct simulation Monte Carlo method (DSMC) [14]. Such molecular beams are of great potential importance for material processing (etching, deposition, etc.), as well as for studying the relaxation processes in gasses and gas–surface collisions. Another possible application of lattice-accelerated beams of neutral particles is rocket propulsion, where high velocities of trapped particles may result in extremely large specific impulses of lattice-driven propulsion devices. At pressures on the order of 1 atm, it is not possible to trap particles and create a molecular beam using a chirped optical lattice. It is possible, however, to transfer the momentum and energy from a traveling optical lattice to the gas; the optimal phase velocity in this case is close to the average gas thermal velocity [13]. Microscale thrusters with typical throat diameters of hundreds of microns to millimeters is one of the possible applications of this type of interaction [14].

The main goal of this paper is to numerically study new propulsion concepts based on the interaction of an optical lattice with gas molecules in two flow regimes, nearly free-molecule and continuum. Two new microthruster schemes are considered for these regimes that use 1) acceleration of molecules to very high velocities with a linearly chirped lattice, and 2) energy and momentum deposition from an optical lattice traveling at a constant speed into the throat of a microscale nozzle. The estimates of thruster performance characteristics are presented and possible ways to improve them are outlined. The direct simulation Monte Carlo method [15] is used in this study.

II. Laser Beam Propulsion

Propulsion concepts based on laser energy deposition, primarily to the solid matter, were proposed as early as 45 years ago. One of the first studies in the field is presented in [16] in which the thrust produced by molecules vaporized from a target surface due to laser radiation was examined. The process of surface ablation and thrust generation by pulsed laser beams has been extensively studied experimentally and theoretically starting in the early 1970s [17,18] for different chemical composition of the surface. The use of laser beam propulsion with a terrestrial source of laser energy was proposed in [18]. More recent research [19] includes the use of high-energy lasers to transmit solar power through free space in the form of coherent light.

The laser ablation of the surface is not the only known laser-based mechanism of spacecraft thrust generation. The laser beam energy may also be used for liquid propulsion thrusters, where the laser energy plays the role of the oxidizer, and for air-driven thrusters [20]. In the latter concept, the thruster is powered by atmospheric air effectively heated by a laser beam. At present, although lasers did not take on a thrust-producing role of ion engines, the idea of beaming energy from both space- and terrestrial-based lasers to power spacecraft continues to draw interest. A radiatively driven hypersonic wind tunnel was proposed 10 years ago [21] to provide high-enthalpy, high-Mach-number, true airflows for durations of seconds with high-power laser or electron beams as suitable energy sources. The concept has recently been demonstrated at 1 MW of electron beam energy power [22].

The principal difference of the present work from previous studies is that the nonresonant impulse and energy deposition are used here. This means that only translational and not internal energies of molecules are directly changed by laser radiation, and it is therefore possible to avoid or minimize a number of undesirable effects, such as molecular dissociation and ionization, and associated charging and degradation of working surfaces.

III. Optical Lattices in Free Molecular and Weakly Collisional Regimes

A periodic optical dipole potential is created by the interaction between a polarizable particle and the field of an optical interference pattern created by counterpropagating laser fields with wave vectors $\boldsymbol{k}_1$ and $\boldsymbol{k}_2$. The phase velocity of the pattern, and therefore the potential, is given by $\xi = (\omega_1 - \omega_2)/q$, where $q = |\boldsymbol{k}_1 - \boldsymbol{k}_2|$.

For laser radiation far from resonance, the ponderomotive force on the molecules within the lattice is given by the quasi-electrostatic approximation [23]

$$F(x,t) = 0.5\alpha\nabla E(x,t)^2$$

It has been shown [12] that the equation of collisionless motion of a particle moving in a pulsed accelerated or decelerated optical lattice is given by

$$\frac{d^2x}{dt^2} = -\frac{\alpha q E_1(t) E_2(t)}{2m}\sin(qx - \beta t^2) = -a\sin(qx - \beta t^2)$$

where E_1 and E_2 are the amplitudes of the electric fields of the two laser beams. Here, the first term of the product represents the maximum force per unit mass supplied by the optical lattice. In a reference frame that accelerates with the optical lattice, this equation may be conveniently rewritten in nondimensional units

$$\frac{d^2\theta}{d\bar{t}^2} = -\frac{aq}{\beta}\sin(\theta) - 2$$

where $\theta = \bar{x} - \bar{t}^2$, $\bar{t} = \sqrt{\beta}t$ and $\bar{x} = qx$. The phase-space analysis [12] shows that particles with velocities and coordinates that satisfy the requirement $|2\beta/aq| < 1$ will be trapped by accelerated lattice, and their velocities increase with the lattice velocity.

With increasing laser beam intensities, the optical lattice potential depth increases and at relatively low gas densities a large number of gas particles can be trapped and collisionlessly accelerated. Particle velocities can be increased from the room level to the 10–100 km/s range in a short laser pulse over distances of hundreds of microns [12]. The evolution of particles that are distributed over a range of velocities, and over all phases, is described by the Boltzmann equation. For short acceleration periods, acceleration without collisions between particles becomes possible at pressures in the 10^4 Pa range, and the collision integral in this equation can be set to zero. The results of calculations of particle acceleration using the solution of the collisionless Boltzmann equation are given in [12]. More details on the physics of the acceleration of the polarizable particles may be found in [24], and particle trajectories in free-molecule and collisional regime are studied in [25].

To model the evolution of particles at higher pressures, when the collision time in gas becomes on the order of the pulse duration and molecular collisions are important, the full integro-differential Boltzmann equation has to be solved. One of the most convenient and widely used approaches to the solution of the Boltzmann equation is the DSMC method. This method has been used in all presented computations. The principal computational tool used in

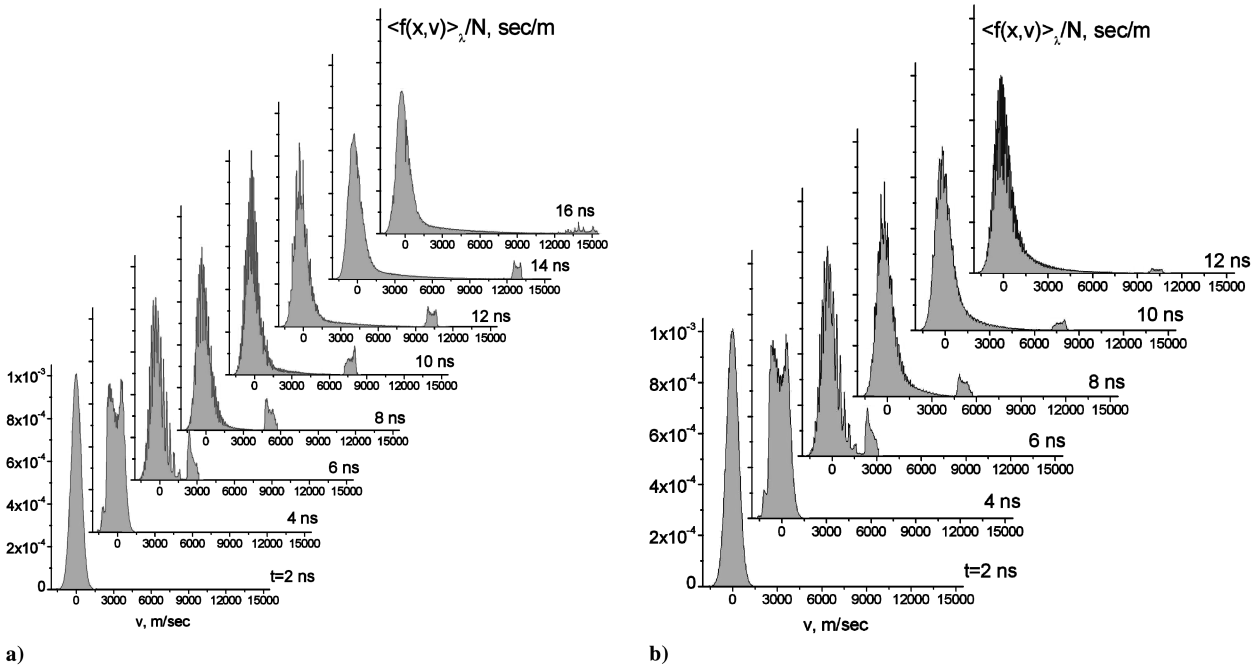

Fig. 1 Distribution function of molecular velocities at different time moments for a) 400 Pa and b) 1300 Pa.

this work is SMILE, an advanced code based on the DSMC method. Details on the tool may be found elsewhere [26]. The variable hard sphere model is used for intermolecular interactions. The discrete Larsen–Borgnakke model with temperature-dependent rotational relaxation number is used for rotation-translation energy transfer.

Modeling of particle acceleration due to the impact of an optical lattice in a weakly collisional regime is performed in one dimension, with periodic boundary conditions applied at the inflow/outflow boundaries. Methane gas, initially stagnant at a temperature of 300 K, is treated as the working fluid. Two gas pressure are considered: 400 and 1300 Pa. The maximum laser beam intensity is assumed to be 6×10^{15} W/m^2, the optical lattice wave length is 400 nm, and a Gaussian temporal profile of intensity is used with a maximum at 10 ns. The computation is performed with about 3 million molecules to provide an acceptable accuracy of the distribution functions, and the computational domain spans over 10 wavelengths. The unsteady flow development is modeled with a time step of 10^{-12} s. The influence of molecular collisions on acceleration is illustrated in Fig. 1, in which the distribution function of molecular velocities in the laser beam direction is shown.

Over the first few nanoseconds, the distribution function is close to Maxwellian because the beam intensity is relatively weak at this stage. Then, by $t = 4$ ns, a bimodal distribution starts to appear. The separation of trapped molecules from untrapped ones becomes clear at times larger than 6 ns. It is also clearly seen that there is a considerable amount of trapped molecules accelerated up to velocities of 15 m/s over the time period of 16 ns for a pressure of 400 Pa. The larger number of molecular collisions at 1300 Pa generally reduces the number of trapped particles, because almost all trapped particles that collide with other particles leave the potential well as the result of collisions. Still, there is a significant amount of molecules accelerated to velocities over 10 km/s, which means that such an acceleration is possible even for collisional gas with pressures on the order of 1300 Pa.

IV. Low-Density Microthruster

The acceleration of molecules to very high velocities, possible when the gas collision time is on the order of or smaller than the pulse duration, may be used in propulsion devices with the primary goal of obtaining high specific impulses. One of the possible designs of this device [14] is shown in Fig. 2. In this figure, the transparent plates denote windows, and gray plates denote mirrors. Carrier gas is

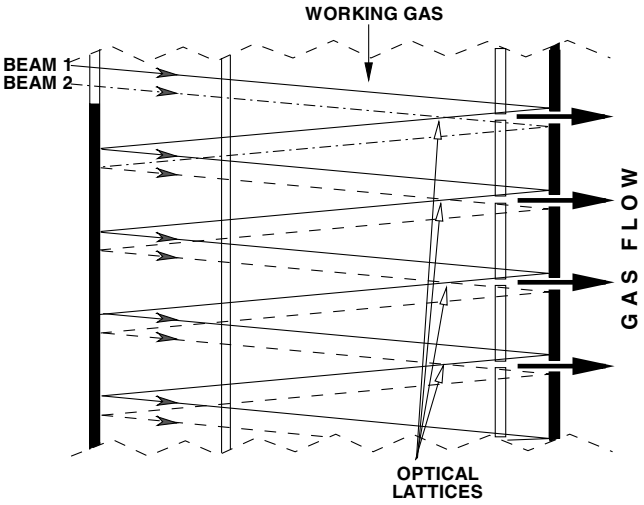

Fig. 2 Schematic of a low-density micropropulsion device powered by the optical lattice/gas interaction.

entrapped between two transparent windows, one of which has multiple openings to allow for gas expansion. The gas density between the mirrors and the windows is negligibly small. The principle of operation is based on acceleration of molecules by multiple optical lattices created with two laser beams that have multiple intersections in the gas section. Gas molecules accelerated to very high velocities leave through the openings, thus creating net thrust force. The left window separates the carrier gas from the left branch of optical lattices, which would have otherwise accelerated molecules in the direction opposite to the openings. The optical lattices are created through multiple reflections of the two counterpropagating beams on the opposite windows. Because of the recent progress in laser related optics technologies, which has resulted in the improved performance of low-absorbing mirrors, reflectivity on the order of 99.999% is now feasible. The advent of ultrahigh reflectivity mirrors, in conjunction with the fact that only a small fraction of the laser energy is absorbed by the gas, makes possible the use of hundreds or even thousands of thrust-producing openings in a single propulsion device fed by two laser beams.

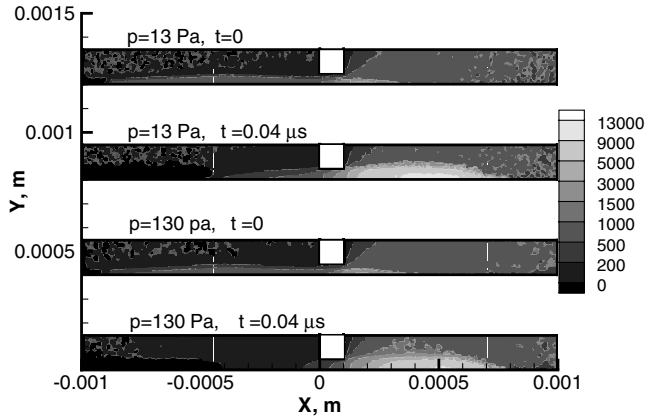

Fig. 3 Axial velocity fields (m/s) in a low-density micropropulsion device at two different pressures and two time moments.

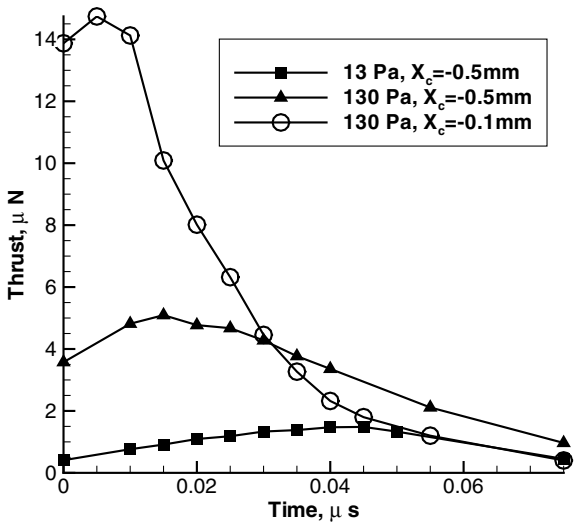

Fig. 4 Temporal change in thrust force for different pressures and center of the lattice locations X_c.

The performance characteristics of the preceding low-density propulsion device has been analyzed with the DSMC method for different stagnation pressures. The simulations have been performed for an axisymmetric domain that represents a part of the flow adjacent to an opening. The computational domain is shown in Fig. 3. The equilibrium stagnation conditions were set at the upstream boundary (left). The lower boundary is the axis of symmetry, and specular conditions are specified at the upper boundary to simulate the effect of a large array of openings. The vacuum condition was used at the downstream boundary. The working gas was methane and the stagnation temperature was 300 K. The three stagnation pressures used were 1.3, 13, and 130 Pa. The optical lattice was created with two 800 nm wavelength 50 μm radius beams with a chirp of 10^{19} rad/s^2; the lattice center was located 0.5 mm upstream from the opening; the maximum laser intensity at the axis was 6.4×10^{16} W/m^2, and the pulse duration was 10 ns. The initial lattice velocity ξ_0 varied from -5 to -7.5 km/s to select the optimum value.

The evolution of the axial flow velocity field after a single pulse is presented in Fig. 3 for pressures 13 and 130 Pa and $\xi_0 = -6.5$ km/s. Two time moments are shown here: $t = 0$, which corresponds to the time immediately after the pulse, and $t = 0.04$ μs. During the pulse, the trapped molecules start moving toward the opening, and the location of the maximum flow velocity shifts downstream by about 0.1 mm by the end of the pulse. The molecules with high velocities start passing through the opening and create a region of elevated velocities next to its exit plane. After 0.04 μs, most of the molecules have passed through the opening and their relatively small radial velocities led to the formation of a high-velocity region closer to the axis downstream from the orifice. For the lower pressure of 13 Pa, the velocities in that region exceed 10 km/s and reach a maximum of 13.5 km/s. The twentyfold increase of average flow velocities in the coreflow after the opening exit plane as a result of the lattice/gas interaction is related both to the high-number flux of the trapped molecules and their low divergence from the centerline. For this pressure, the mean free path is larger than the distance from the center of the lattice to the exit plane, and molecular collisions do not reduce significantly the number of particles trapped by the optical lattice. For the higher pressure of 130 Pa, the molecular collisions visibly reduce the number of trapped particles, therefore decreasing the average velocity in the high-velocity region at and after the exit plane.

The temporal change of the thrust force computed using instantaneous values of flow velocity and density are given in Fig. 4 for pressures 13 and 130 Pa. It is clearly seen that the thrust force has a maximum at about 0.04 μs for 13 Pa and 0.02 μs for 130 Pa. The value of 0.04 μs corresponds to the time when the trapped molecules initially located at the center of the lattice reach the orifice exit plane. For $p = 130$ Pa, the mean free path is too small for these molecules to travel to the exit plane without collisions, and the largest contribution to the thrust force give trapped molecules located closer to the exit plane. The center of the lattice generally corresponds to the maximum laser intensity, and therefore the largest portion of trapped molecules compared with the regions off-center. It is therefore beneficial for the higher pressure to move the center of the lattice closer to the exit plane. Even though the number density is somewhat smaller in that region compared with the stagnation conditions, it results in a significantly larger number of trapped molecules that reach the exit plane compared with the original location. This is illustrated in Fig. 4 for the optical lattice center located at $X_c = -0.5$ mm and $X_c = -0.1$ mm. Note, the maximum thrust in the latter case is about 10 times higher than that for 13 Pa.

For pressures lower than 13 Pa, the thrust as a function of time increases almost linearly with pressure, as shown in Table 1. It is also possible to preserve this linear behavior even for higher pressures, by moving the center of the lattice closer to the exit plane. The increase of thrust due to the optical lattice is very significant; about 20 times for the range of pressures considered. The maximum specific impulse observed is about 450 s, which is a sevenfold improvement compared with the flow not affected by the optical lattice. Note also that the results shown are for the initial lattice velocity of -6.5 km/s, which was found to give maximum particle trapping. This is because at time 10 ns, which corresponds to the maximum of the laser intensity, the lattice velocity is about zero and therefore the maximum number of molecules become trapped. For lattice velocities of -5 and -7.5 km/s, the maximum thrust decreases by over 40% compared with the -6.5 km/s case.

V. Energy and Momentum Deposition in the Continuum and Transitional Regimes

When the gas density is high enough so that the mean collision time is much smaller than the pulse duration, it is not possible to effectively trap particles and accelerate them to high velocities with the lattice; it is still possible, however, to increase the particle thermal velocity as well as transfer momentum from the lattice to the gas. In this case, the chirping of the lattice is not needed, and a constant lattice velocity should be used. Let us now consider the effect of

Table 1 Maximum observed thrust and specific impulse for various pressures and X_c

Pressure, Pa	X_c, mm	Mass flow, kg/s	Thrust, N	I_{sp}, s
1.3	−0.5	3.899×10^{-11}	1.794×10^{-7}	469
13	−0.5	3.400×10^{-10}	1.472×10^{-6}	441
130	−0.5	1.670×10^{-9}	5.092×10^{-6}	311
130	−0.3	2.443×10^{-9}	9.174×10^{-6}	383
130	−0.1	3.360×10^{-9}	1.474×10^{-5}	448

lattice on gas and associated energy deposition in more detail. In what follows, it is assumed that $l_c/\lambda \ll 1$.

In a single interaction of a molecule with the lattice potential, the change in momentum and energy of the molecule are given by $\Delta p = 2m(\xi - v)$, $\Delta\varpi = 2m(\xi - v)\xi$. In the collisionless case, the corresponding trajectory length for the momentum or energy exchange with the moving potential well is about λ. In a high-density gas, a particle travels only a small part of its trajectory, approximately l_c/λ, over a collision time given by $\tau_{\text{col}} = l_c/|v - \xi|$. Therefore, the effective rates of momentum and energy exchange are

$$\dot{\Delta p} \sim (\Delta p/\tau_{\text{col}})l_c/\lambda = 2m(\xi - v)|\xi - v|/\lambda$$

and

$$\dot{\Delta\varpi} \sim (\Delta\varpi/\tau_{\text{col}})l_c/\lambda = 2m\xi(\xi - v)|\xi - v|/\lambda$$

Integrating these expressions with the Maxwellian distribution function over velocity space from $\xi - \Delta$ to $\xi + \Delta$ for all particles inside the potential well, and expanding the distribution function into a Taylor series up to the first order, $f(v) \approx f_0(\xi) + (df_0/dv)(v - \xi)$, we obtain the total rate of energy and momentum exchange between the optical lattice and gas given by

$$\dot{W} = -P_d \sim -\frac{m^2\xi^2}{\lambda k_B T} f_0(\xi)\Delta^4 \tag{1}$$

$$\dot{\Theta} \sim \frac{1}{\xi} P_d = \frac{m^2\xi}{\lambda k_B T} f_0(\xi)\Delta^4 \tag{2}$$

where

$$W = \frac{\varepsilon_0 E^2}{2} = \frac{I}{c}, \qquad P_d = -\frac{dW}{dt}$$

is the power transferred to the gas due to the optical wave dissipation [13], $\Delta = \sqrt{2\phi_m/m}$, and ϕ_m is the potential well depth. Note that in [13], the coefficient l_c/λ in the corresponding equation for $\dot{W}$ was mistakenly omitted. For two counterpropagating laser beams with the combined intensity $I = I_1 + I_2$, the maximum potential well depth is $\phi_m = \alpha I Z_0/n$, where $Z_0 = \sqrt{\mu_0/\varepsilon_0} = 376.73\ \Omega$. From Eqs. (1) and (2) follows [13] that the phase velocity, corresponding to the maximum rate of momentum transfer is $\xi^m_{\max} = \sqrt{k_B T/m}$, and the maximum rate of energy transfer is at $\xi^E_{\max} = \sqrt{2k_B T/m}$. It may also be shown that $P_d \propto \dot{\Theta} \propto NI^2$.

Note also that the longitudinal force acting on the gas is $F_x = \dot{\Theta}$. If gas is moving along the optical lattice axis with the velocity v_x, the corresponding F_x and P_d are

$$P_d \sim \frac{m^2(\xi - v_x)^2}{\lambda k_B T} f_0(\xi - v_x)\Delta^4$$

$$F_x \sim \frac{m^2(\xi - v_x)}{\lambda k_B T} f_0(\xi - v_x)\Delta^4$$

and the optimum phase velocities for the energy and momentum transfer from the traveling optical lattice to gas molecules are $\xi^E_{\max} = \sqrt{2k_B T/m} + v_x$ and $\xi^m_{\max} = \sqrt{k_B T/m} + v_x$. For a stagnant gas of methane at 300 K, $\xi^E_{\max}$ and $\xi^m_{\max}$ correspond to 558 and 394 m/s, respectively. To verify these analytical predictions and provide more detail on energy and momentum deposition, one-dimensional DSMC computations have been performed for the following laser parameters. The laser pulse duration was 1 ns, the maximum single laser beam intensity was 0.25×10^{17} W/m^2 and 0.5×10^{17} W/m^2, the optical lattice wave length was 400 nm, and a Gaussian temporal profile of intensity was used with a maximum at 1 ns. The lattice velocity was varied from 0 to 1500 m/s. Again, the working gas was methane with $T_0 = 300$ K, and four pressures from 400 to 10^6 Pa were considered.

The energy and momentum deposition per molecule is presented in Fig. 5 as a function of the lattice velocity for $I_{\max} = 0.5 \times 10^{17}$ W/m^2. Note that the energy values are divided by the Boltzmann constant, and the momentum is divided by the molecular mass. Several conclusions can be drawn from these figures. First, the values of $\xi^E_{\max}$ and $\xi^m_{\max}$ are close to those predicted analytically (compare the maxima in Fig. 5 to 558 and 394 m/s, respectively). Second, the energy, as well as momentum, deposition per molecule slightly increases with pressure, whereas the theory predicts a linear dependence on N ($P_d \propto NI^2$). This small difference is related to the fact that the theory does not include all the details of the interactions between the molecules inside and outside the potential well, when some molecules may leave the well while others may become trapped in the well due to molecular collisions. The third conclusion is that the energy and momentum deposition are generally less efficient for 10^6 Pa than for lower considered pressures at high lattice velocities. This is related to the fact that the quick Maxwellization at 10^6 Pa, when the collision time is over an order of magnitude shorter than the pulse duration, acts to prevent the deposition as compared with the velocity distribution that has a plateau formed due to the optical Landau damping [13] at lower pressures. This is confirmed by the fact that deposition at high lattice velocities becomes relatively more efficient for shorter pulses.

The energy and momentum deposition for a smaller laser intensity are presented in Fig. 6. The general shape of the lattice velocity, as well as pressure dependence, is similar to that of a higher intensity. However, the absolute values are significantly lower for this case. The energy deposition per molecule is smaller by about a factor of two for lower pressures and four for high pressures, whereas the

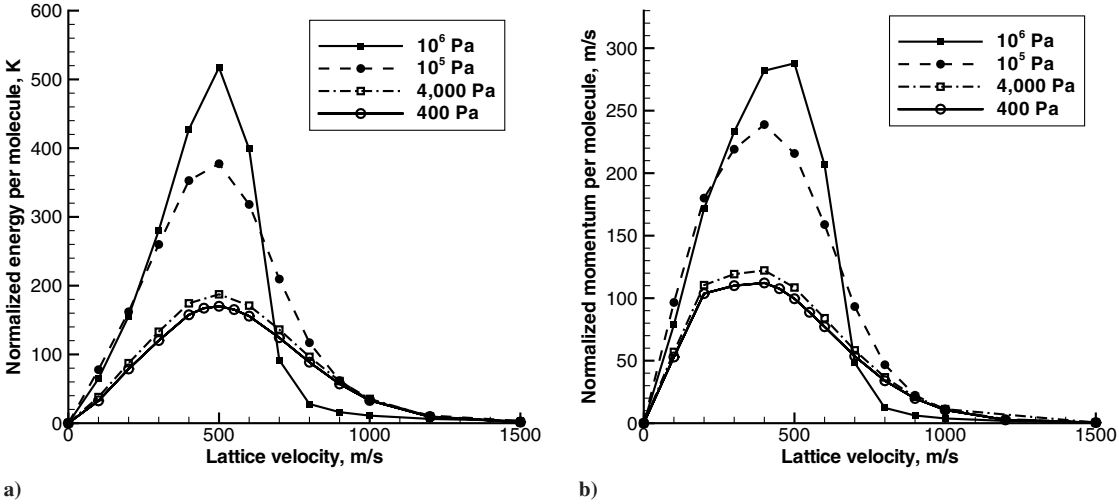

a) b)

Fig. 5 Deposition of a) energy and b) momentum in an initially stagnant gas for different pressures and $I_{\max} = 0.5 \times 10^{17}$ W/m^2.

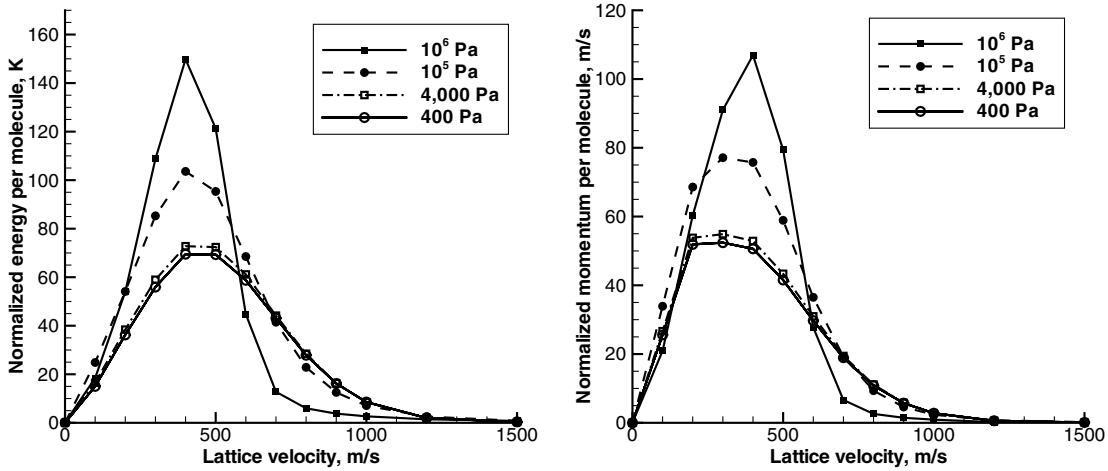

a) b)

Fig. 6 Deposition of a) energy and b) momentum in an initially stagnant gas for different pressures and $I_{max} = 0.25 \times 10^{17}$ W/m^2.

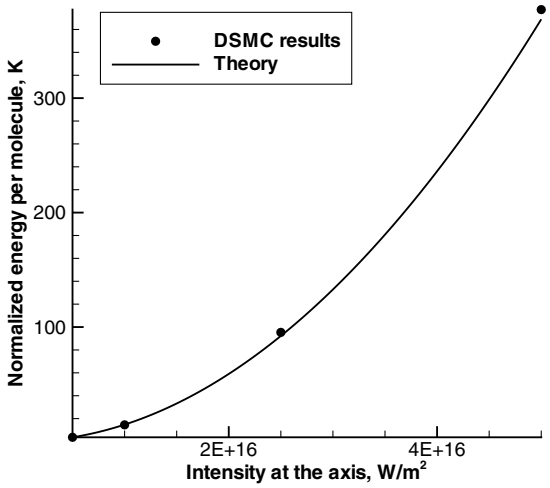

Fig. 7 Energy deposition for different laser intensities.

momentum deposition is about two times smaller for $I_{max} = 0.25 \times 10^{17}$ W/m^2. Note that for high pressures, the energy deposition as a function of laser intensity is in good agreement with the theory that predicts that I^2 dependence. It is also clearly seen in Fig. 7, in which the energy deposition is shown for gas pressure of 10^5 Pa and lattice velocity of 500 m/s. The line in this figure represents $\bar{E}(I_{0,max})$ $(I_{max}/I_{0,max})$, where $I_{0,max} = 0.25 \times 10^{17}$ W/m^2.

VI. High-Density Microthruster

The nonresonant deposition of laser radiation energy into high-density gas with the consequent increase of both gas momentum and energy, examined in the previous section, may be used to construct a thruster driven by the nonresonant optical lattice/gas interaction. Although there are a number of possible configurations for such a thruster, the most straightforward seems to be a converging–diverging de Laval nozzle with the interaction region located near the nozzle throat. A schematic of such a configuration is shown in Fig. 8. The first laser beam passes through the plenum and the diverging section of the nozzle, and then reflects back on the mirror mounted on the upper part of the nozzle. The second beam enters the diverging section through the exit plane after reflecting on the mirror located in the lower part of the nozzle, and intersects with the first beam near the nozzle throat, thus creating an optical lattice in that region. Because the energy consumed by gas molecules over a single pulse represents a small fraction of the total pulse energy, the beams should be reused using a mirror system, with an optical lattice repeatedly formed in the throat region.

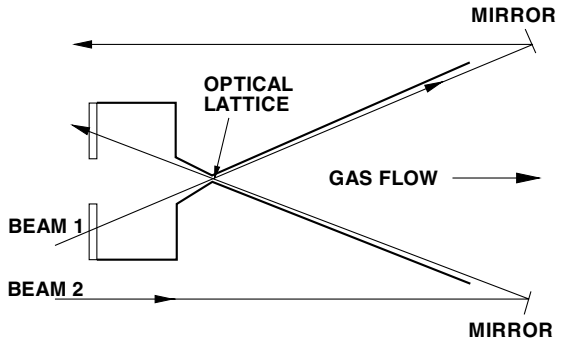

Fig. 8 Schematic of microthruster integrated with an optical lattice, operating in the continuum regime.

The efficiency of the proposed scheme has been studied for a cold gas microthruster influenced by intersecting 690 nm laser beams with a pulse duration on the order of 5×10^{-11} s, maximum intensity at the axis of 5×10^{17} W/m^2, a beam radius of 40 μm, and the initial lattice velocity of 1300 m/s. The ten 20 ns pulses were repeated every 30 ns, and such a high repetition rate may be achieved with the aforementioned multiple use of the laser pulse power. A conical de Laval nozzle was used with the throat radius of 50 μm, the length of the diverging part of 1 mm, and the diverging half-angle of 15 deg. The stagnation pressure was assumed to be 10^5 Pa, temperature was 300 K, and the carrier gas was nitrogen. For this pressure, the considered laser pulse is well below the breakdown [27].

The results of the unsteady flow development after 10 successive laser pulses are shown in Fig. 9 for the axial velocity and translational temperature fields. Immediately after the pulses, $t = 0$, there is a high-velocity region (Fig. 9, left) observed at the location of the optical lattice near the nozzle throat. The maximum velocity reaches 2500 m/s in this region, compared with about 400 m/s if there were no optical lattice. The velocity perturbation propagates downstream, and the elevated velocity front spreads from the nozzle centerline out to the nozzle surface. The velocity maximum in this front decreases with time and leaves the nozzle after 1 μs from the pulses. The gas translational temperature (Fig. 9, right) also increases due to the lattice/gas interaction. Initially ($t = 0$), the temperature in the throat is approximately 700 K, which is about 450 K higher than in the flow without the lattice. During the subsequent propagation of the elevated temperature front through the diverging part of the nozzle, the maximum temperature is observed near the surface and not at the nozzle axis. This observation is due to the friction of the high-energy front on the diffuse wall. The gas temperature in that region is typically about 200 K higher than the surface temperature of 300 K, which is an indication that the surface may be exposed to significant

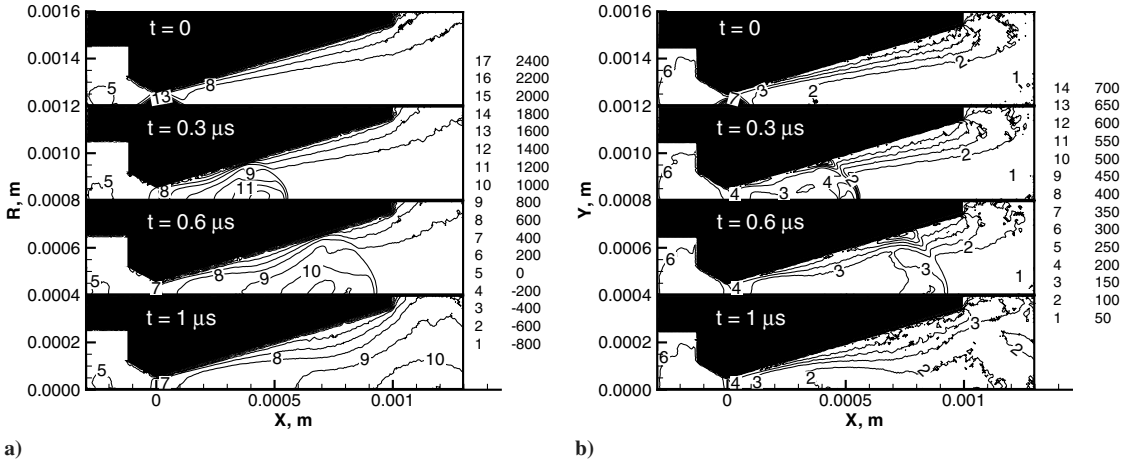

Fig. 9 Temporal evolution of the axial velocity fields (m/s) inside a micronozzle: a) axial velocity, m/s; b) translational temperature, K.

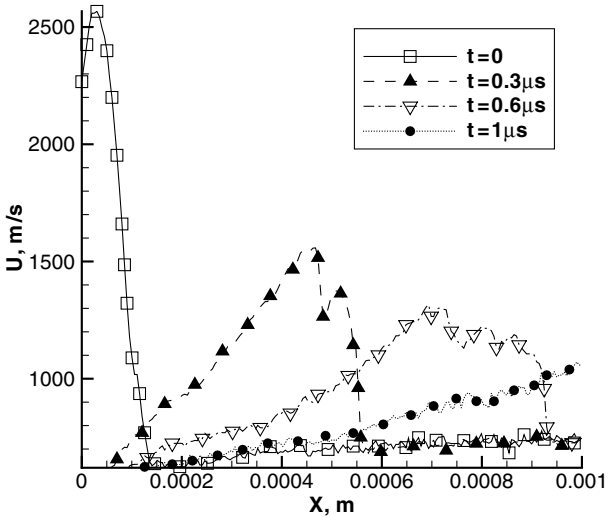

Fig. 10 Axial velocity profiles along the nozzle axis at different time moments.

loads as the heated front passes through the diverging part of the nozzle.

The temporal change of the axial velocity profile extracted along the nozzle axis is presented in Fig. 10. In this figure, $X = 0$ and $X = 1$ mm correspond to the nozzle throat and exit planes, respectively. Although most of the velocity increase due to the lattice–gas interaction occurs downstream from the throat, there is a significant part of molecules being accelerated by the lattice in the converging section of the nozzle, where the flow is subsonic. This perturbation is therefore expected to affect both the nozzle mass flow rate and the thrust. Positioning the lattice fully in the supersonic region further downstream would minimize the impact of the lattice on the mass flow, but on the other hand, reduce the momentum and energy deposition into the gas. Generally, at high pressures, the energy deposition increases nearly as the square of the gas density, and the interaction of the lattice with a higher-density gas near the throat is thus beneficial.

The axial velocity maximum at the axis decreases from over 2500 m/s at $t = 0$ to about 1500 m/s at 0.3 μs and further down to 1300 m/s at 0.6 μs. The half-velocity front reaches the nozzle exit at $t \approx 0.65$ μs. After 1 μs, the front has mostly left the nozzle, but the velocity at the exit plane is still over 300 m/s higher than for an undisturbed flow. The large values of axial velocity at the exit result in an almost threefold increase in thrust due to the lattice–gas interaction. The thrust of the nozzle increases from 1.19 mN for a flow without a lattice to 2.99 mN for the flow. The lattice effect on the specific impulse is smaller because the mass flow also increases in the present configuration, but still significant, 92 s vs 72 s. The better performance of a cold gas thruster integrated with an optical lattice demonstrates the feasibility of such an integration. It is also important that larger gas density, laser energy, and the number of pulses will all result in a subsequent increase in device performance both in terms of thrust and specific impulse. Because only a small fraction of laser energy, about 10^{-6}, is transferred to gas, multipass systems may be used to effectively recycle laser beams to produce a number of optical lattices separated in time.

Note also that although a microscale, 100 μm throat diameter, thruster was considered in this research, the approach and the conclusions are fully applicable for larger scale thrusters.

VII. Conclusions

The nonresonant interaction of gas molecules with the optical lattice potential is studied with application to rocket propulsion. Two propulsion concepts are examined, high density and low density, based on the gas flow regime. The direct simulation Monte Carlo method is used in all presented computations.

The principal driving force for the nonresonant laser propulsion at high densities is the energy and momentum deposition from optical lattice to gas. An analytical model has been developed to qualitatively characterize this deposition; the results of the model are in good agreement with the DSMC predictions. Note that the analytical model may be used to specify initial conditions for optical lattice/gas interactions in the continuum regime using continuum approaches, such as the solution of Navier–Stokes equations.

The high-density propulsion device considered in this work represents a de Laval nozzle with power deposition in the region of the nozzle throat. The stagnation pressure of 10^5 Pa was considered, and the DSMC computations of a 1 mm long nozzle have shown an improvement of about 300% in thrust and 20% in specific impulse for a $\sim$50 mJ pulse. It is possible to use higher pressures and larger nozzle dimensions to increase the thrust and specific impulse. It is also beneficial to recycle the laser beams using mirrors and an optical cavity, because the laser energy absorption by gas is very small, on the order of 10^{-6} for a pressure of 10^5 Pa.

The nonresonant acceleration of molecules to velocities of 10 km/s and higher in a chirped frequency optical lattice is used in the proposed low-density propulsion device. The stagnation pressures from 1.3 to 130 Pa are investigated, and a sevenfold increase in the specific impulse is obtained. The maximum thrust and specific impulse for 130 Pa are 16 μN and 448, respectively. There are a number of possible ways to increase these numbers, such as to 1) increase stagnation pressure; 2) use larger lasers and bigger openings; 3) use a multiple-opening configuration to recycle laser power; 4) optimize the device in terms of lattice location, chirp, and velocity; 5) use polar molecules, such as H_2O. The latter option alone may give several times larger specific impulse due to the larger forces on molecules.

The shown ability of the optical lattice to accelerate molecular beams to extremely high velocities in weakly collisional regimes without ionization and dissociation of molecules may be used not only in propulsion, but also in various material processing devices. The nonresonant energy deposition at high pressures may also be used to create high-temperature gas pockets in arbitrary points of space. Note that a variable lattice velocity needs to be used for this purpose to account for gas temperature increase and provide optimum energy deposition.

Acknowledgments

The authors would like to thank Ingrid Wysong, Andrew Ketsdever, and Peter Barker for many helpful discussions. Sergey F. Gimelshein acknowledges the encouragement and support from the Air Force Research Laboratory, Propulsion Directorate.

References

[1] Schiffer, M., Rauner, M., Kuppens, S., Zinner, M., Sengstock, K., and Ertmer, W., "Guiding, Focusing, and Cooling of Atoms in a Strong Dipole Potential," *Applied Physics B (Lasers and Optics)*, Vol. 67, No. 6, 1998, pp. 705–708. doi:10.1007/s003400050569

[2] Stamper-Kurn, D. M., Andrews, M. R., Chikkatur, A. P., Inouye, S., Miesner, H. J., Stenger, J., and Ketterle, W., "Optical Confinement of a Bose-Einstein Condensate," *Physical Review Letters*, Vol. 80, No. 10, 1998, pp. 2027–2030. doi:10.1103/PhysRevLett.80.2027

[3] Renn, M. J., Montgomery, D., Vdovin, O., Anderson, D. Z., Wieman, C. E., and Cornell, E. A., "Laser-Guided Atoms in Hollow-Core Optical Fibers," *Physical Review Letters*, Vol. 75, No. 18, 1995, pp. 3253–3256. doi:10.1103/PhysRevLett.75.3253

[4] Karczmarek, J., Wright, J., Corkum, P., and Ivanov, M., "Optical Centrifuge for Molecules," *Physical Review Letters*, Vol. 82, No. 17, 1999, pp. 3420–3423. doi:10.1103/PhysRevLett.82.3420

[5] Livingston, M. S., and Blewett, J. P., *Particle Accelerators*, McGraw–Hill, New York, 1962.

[6] Neely, A. J., and Morgan, R. J., "Superorbital Expansion Tube Concept, Experiment And Analysis," *Aeronautical Journal*, Vol. 98, 1994, p. 97.

[7] Kazantsev, A. P., "Acceleration of Atoms by Light," *Soviet Physics–JETP*, Vol. 39, No. 4, 1974, pp. 784–789.

[8] Kazantsev, A. P., "Resonance Light Pressure," *Soviet Physics–Uspekhi*, Vol. 21, No. 1, 1978, pp. 58–76. doi:10.1070/PU1978v021n01ABEH005509

[9] Corkum, P. B., Ellert, C., Mehendale, M., Dietrich, P., Hankin, S., Aseyev, S., Rayner, D., and Villeneuve, D., "Molecular Science with Strong Laser Fields," *Faraday Discussions*, Vol. 113, 1999, pp. 47–59. doi:10.1039/a903428e

[10] Madison, K. W., Bharucha, C. F., Morrow, P. R., Wilkinson, S. R., Sundaram, Q. N. B., and Raizen, M. G., "Quantum Transport of Ultracold Atoms in an Accelerating Optical Potential," *Applied Physics B (Lasers and Optics)*, Vol. 65, No. 6, 1997, pp. 693–700. doi:10.1007/s003400050335

[11] Peik, E., Ben Dahan, M., Bouchoule, I., Castin, Y., and Salomon, C., "Bloch Oscillations and an Accelerator for Cold Atoms," *Applied Physics B (Lasers and Optics)*, Vol. 65, No. 6, 1997, pp. 685–692. doi:10.1007/s003400050334

[12] Barker, P. F., and Shneider, M. N., "Optical Microlinear Accelerator for Molecules and Atoms," *Physical Review A*, Vol. 64, No. 3, 2001, p. 033408. doi:10.1103/PhysRevA.64.033408

[13] Shneider, M. N., and Barker, P. F., "Optical Landau Damping," *Physical Review A*, Vol. 71, No. 5, 2005, p. 053403. doi:10.1103/PhysRevA.71.053403

[14] Shneider, M. N., Gimelshein, S. F., and Barker, P. F., "Development of Efficient Micropropulsion Devices Based on Molecular Acceleration in Pulsed Optical Lattices," *Journal of Applied Physics*, Vol. 99, 2006, p. 063102. doi:10.1063/1.2183410

[15] Bird, G. A. *Molecular Gas Dynamics and the Direct Simulation of Gas Flows*, Clarendon Press, Oxford, England, U.K., 1994.

[16] Askaryan, G. A., "Effects of the Gradient of Strong Electromagnetic Beam on Electrons and Atoms," *Soviet Physics—JETP*, Vol. 15, No. 6, 1962, pp. 1088–1090.

[17] Prokhorov, A., Batanov, V., Bunkin, F., and Fedorov, V., "Metal Evaporation Under Powerful Optical Radiation," *IEEE Journal of Quantum Electronics*, Vol. 9, No. 5, 1973, pp. 503–510. doi:10.1109/JQE.1973.1077511

[18] Pirri, A. N., Monsler, M. J., and Nebolsine, P. E., "Propulsion by Absorption of Laser Radiation," *AIAA Journal*, Vol. 12, No. 9, 1974, pp. 1254–1261.

[19] Smith, M. H., Fork, R. L., and Cole, S. T., "Safe Delivery of Optical Power from Space," *Optics Express*, Vol. 8, No. 10, 2001, pp. 537–546.

[20] Bunin, F. V., and Prokhorov, A. M., "Use of Laser Power Source to Create Thrust," *Uspekhi Fizicheskikh Nauk (Soviet Physics–Uspekhi)*, Vol. 119, No. 3, 1976, pp. 425–446.

[21] Miles, R. B., Brown, G. L., Lempert, W. R., Yetter, R., Williams, G. J., Bogdanoff, S. M., Natelson, D., and Guest, J. R., "Radiatively Driven Hypersonic Windtunnel," *AIAA Journal*, Vol. 33, No. 8, 1995, pp. 1463–1470.

[22] Girgis, I. G., Brown, G. L., Miles, R. B., and Lipinski, R. J., "Fluid Mechanics of a Mach 8–12, Electron Beam Driven, Missile-Scale Hypersonic Wind Tunnel: Modeling and Predictions," *Physics of Fluids*, Vol. 14, No. 11, 2002, pp. 4026–4039. doi:10.1063/1.1501826

[23] Boyd, R. W., *Nonlinear Optics*, Academic Press, Boston, 1992.

[24] Shneider, M. N., Gimelshein, S. F., and Barker, P. F., "Transport in Room Temperature Gases Induced by Optical Lattices," *Journal of Applied Physics*, Vol. 100, 2006, p. 074902. doi:10.1063/1.2355447

[25] Ngalande, C., Shneider, M., and Gimelshein, S., "Collisional Molecular Transport in Pulsed Optical Lattices," *37th AIAA Plasmadynamics and Lasers Conference*, AIAA Paper 2006-2900, June 2006.

[26] Ivanov, M. S., Markelov, G. N., and Gimelshein, S. F., "Statistical Simulation of Reactive Rarefied Flows: Numerical Approach and Applications," AIAA Paper 98-2669, June 1998.

[27] Dewhurst, R. J., "Comparative Data on Molecular Gas Breakdown Thresholds in High Laser-Radiation Fields," *Journal of Physics D: Applied Physics*, Vol. 11, No. 16, 1978, pp. L191–L195. doi:10.1088/0022-3727/11/16/002

A. Gallimore
Associate Editor